Transactions, SMiRT-22
San Francisco, California, USA - August 18-23, 2013
Division IX (include assigned division number from I to X)

DAMAGE ASSESSMENT OF INTERIM DRY STORAGE CASKS FOR SPENT NUCLEAR FUEL

Giovanna Xotta[1], Kaspar Willam[2], Bora Gencturk[3] and Yumping Xi[4]

[1]Post Doc, Dept. of Civil and Environmental Engineering, Univ. of Houston, TX (giovanna.xotta@dicea.unipd.it)
[2]Professor, Dept. of Civil and Environmental Engineering, University of Houston, TX
[3]Assistant Professor, Dept. of Civil and Environmental Engineering, University of Houston, TX
[4]Professor, Dept. of Civil, Environmental, and Architectural Engineering, University of Colorado at Boulder, CO

ABSTRACT

This paper addresses different degradation mechanisms in spent nuclear fuel casks made of a concrete outer pack and a steel liner considering realistic environmental and mechanical load histories.

To this end a model cask is examined computationally in form of coupled hygro-thermo-mechanical finite element studies of the underlying mechanical and diffusive transport properties. An accelerated aging program is used to determine environmental degradation mechanisms in form of multiphysics simulations which induce progressive damage under sustained mechanical, thermal, and hygral load histories, and which include chemical effects in form of alkali aggregate reaction.

For this purpose the coupled thermo-hygro-mechanical finite element code developed at Padua University, called NEWCON3D, which treats concrete as a multiphase system, will be updated in order to take into account the chemical effects of alkali silica reaction, ASR. The so enhanced code will find application in the study of spent nuclear fuel casks subjected to accelerated aging in order to predict their long-term performance up to 100 years and more.

INTRODUCTION

Due to the large production of spent nuclear fuel (67,500 metric tons) by the nuclear industry in the United States in the last 40 years, and according to the predictions by the Nuclear Energy Institute of an increase of over 2,000 metric tons per year, the number of Dry Cask Storage Systems (DCSS) for SNF storage capacity will increase drastically in the absence of a long-term nationwide storage facility. These casks are cylindrical structures approximately 6m in height and 3.5m in diameter, with typically 0.6m of concrete shielding walls, placed on concrete pads in an upright position or stacked horizontally. For this reason a comprehensive study of dry casks behavior is warranted in order to fully understand their performance under realistic environmental and mechanical load histories for several hundred of years.

The work presented in this paper, takes inspiration by an ongoing project which aims at developing a probabilistic multi-hazard assessment framework for dry cask storage systems and at performing a comprehensive engineering simulation-based assessment of multiple risks under combined earthquake loads and aging induced deterioration.

This paper will focus attention on the numerical modeling of the DCSS behavior and subsequent degradation, when subjected to realistic load scenarios for 40 years under thermal, hygral and self-weight loadings. Additionally, the Alkali-Silica Reaction (ASR) in concrete will be discussed, that is a deleterious chemical reaction that can produce expansive stresses and so generate microcracks in cement-based materials. This chemical process is critical because DCSS are very susceptible to this chemical degradation if the concrete outer-pack contains reactive-aggregates, such as the ones present in Texas, and if they will be located near coastal regions, where the high moisture level in concrete is a necessary condition for the formation of ASR gel and consequent crack expansion. For the engineering simulations the coupled thermo-hygro-mechanical finite element code NEWCON3D, which treats concrete as a

multiphase system, was adopted and is being further extended in order to take into account the ASR reactions and their effect on mechanical degradation in form of elastic continuum damage.

The goal of the study is to establish a fuller understanding of how the mechnical and environmental load histories affect the long-term performance of dry casks and how they may accelerate the `natural' aging processes.

ACCELERATED AGING DUE TO TEMPERATURE AND RELATIVE HUMIDITY

Environmental effects such as temperature and relative humidity can accelerate the aging of concrete materials due to many chemical processes, such as ASR (discussed in the next section), chloride penetration and carbonation.

With regard to ASR, the role of the water is fundamental because: - a certain internal humidity is necessary for any dissolution, reaction, and formation of amorphous gel and precipitates as it brings into contact the involved reactants; - the gel expansion is governed by water imbibition and, - is necessary for the reaction to continue (see Bazănt and Steffens, 2000; Steffens et al., 2003). Moreover ASR mechanisms are thermoactivated; that is, the higher the temperature, the faster the chemical reactions proceed. This kinetic effect of temperature on ASR results from the thermoactivation of the dissolution of reactive silica at the aggregate-cement interface and the reaction product formation (see Ulm et al., 2000).

One other chemical process that can be deleterious for reinforced concrete, especially if located close to the maritime environments, is chloride penetration. In fact chloride ions, in this condition, may penetrate from seawater into concrete and destroy the passive layer of reinforced concrete if the critical chloride concentration level is reached. This leads to the development of corrosion products at the interface between the steel and embedding concrete, while the volumetric expansion of the rust leads to cracking. Furthermore, reduction of cross-sectional area of steel bars may significantly reduce the load-bearing capacity of the structure. In short, elevated temperatures accelerate the chloride penetration process significantly (see Isteita, 2009).

Finally, carbonation is a chemical process characterized by the reaction of calcium hydroxide with carbon dioxide that results in the formation of calcium carbonate and water. The main consequence of carbonation is the drop of the pH-value of the pore solution of concrete from the standard values between 12.5 and 13.5, to a value of about 8.3 in the fully carbonated zones, so that the passive layer that usually covers and protects the reinforcing steel against corrosion becomes no longer stable. This phenomenon, is also strongly influenced by temperature and humidity; in fact elevated temperatures will accelerate the process while the most dangerous range of external relative humidity for carbonation ranges from 40 to 80 % RH, since the carbonation reaction calls for the presence of water, while under higher atmospheric humidity the diffusion of carbon dioxide is inhibited by the water filling the pore space (Saetta et al., 1993; Salomoni et al., 2007).

ALKALI SILICA REACTION IN CONCRETE MATERIALS

One of the most important causes of deterioration of concrete structures is due to the alkali-silica reaction (ASR), which is the most common form of alkali-aggregate reaction (AAR). This is a chemical reaction that occurs between reactive forms of silica in the aggregates and alkali and hydroxyl ions in the pore solution

This phenomenon was firstly observed by Stanton in 1940, while analysing cracking of structures. He attributed the reason of deterioration to a chemical reaction between cement and aggregate.

In order to reach a better comprehension of the overall process, not fully understood, during the last decades and thanks to the upgraded computational resources, many different and more complex models have been developed. Recalling some of the most important ones: the mesoscopic model based on fracture mechanics approach presented by Bazănt and Meyer, 2000 together with the one for the kinetic of the reaction and the diffusion processes by Bazănt and Steffens, 2000; the thermo-chemo-mechanical

model of the material swelling by Ulm et al., 2000 in the framework of chemo-elasticity; the coupled chemo-hygro-mechanical model, within the framework of porous media, by Bangert et al., 2004; the chemo-thermo-damage model proposed by Comi et al., 2009 and the chemo-hygro-thermo-mechanical model by Pesavento et al., 2012 at variable hygro-thermal conditions.

ASR is a two-stage process: during the first stage, the silica is dissolved from the aggregates forming an amorphous gel and precipitates; during the second stage, the amorphous gel, strongly hydrophilic, swells by imbibition of water and, after filling up the available pore space, creates an increasing internal pressure resulting in pervasive microcracking and a drastic reduction of the mechanical properties.

The multiple processes during the first stage may be described by a single overall chemical reaction, which follows a first-order kinetic law (Dron and Brivot, 1992; Dron and Brivot, 1993). So, introducing a non-dimensional reaction metric $\xi \in [0, 1]$ as a chemical state variable (where ξ=0 represents the beginning and ξ=1 the end of the reaction), the kinetics of the dissolution process may be expressed in the following form:

$$\dot{\xi} = \frac{1-\xi}{\tau_r} \tag{1}$$

where τ_r is the characteristic time for the overall reaction that is humidity and temperature dependent (Ulm et al., 2000; Steffens et al., 2003).

The second stage, specifically the water absorption and gel expansion, may be modeled as proposed by Steffens et al., assuming isotropic deformations ε_{ASR} due to the gel expansion and assuming the following formulation for its evolution:

$$\dot{\varepsilon}_{ASR} = \frac{\alpha \quad \dot{m}_{ASR}}{\rho_{ASR}} \; \boldsymbol{I} \tag{2}$$

where α is the chemo elastic dilation coefficient, ρ_{ASR} is the mass density of the swollen gel and $\dot{m}_{ASR}$ is the increase in mass of the swollen gel, that can be assumed equivalent to the mass of water m_w combined to the amorphous gel. Furthermore the water combination is characterized by an aging process γ that relates the rate of the combined water $\dot{m}_w$ with the reaction rate $\dot{\xi}$.

The aging process, in analogy with the first order kinetic law to describe the dissolution, may be described by the expression:

$$\dot{\gamma} = \frac{1-\gamma}{\tau_a} \tag{3}$$

where γ is the metric of the normalized aging (γ=0 for a just formed gel and γ=1 if it is totally aged) and where τ_a is the characteristic time of the aging process.

Finally, to take into account the effects of micro cracking due to the degradation of the material properties caused by ASR, a scalar chemical damage parameter *V* (Pesavento et al., 2012) may be considered:

$$V = 1 - \frac{E\left(\varepsilon_{ASR}^{vol}, 0\right)}{E_0} \tag{4}$$

where $E\left(\varepsilon_{ASR}^{vol}, 0\right)$ is the elastic modulus after chemical deterioration by ASR, but with no mechanical damage, and where E_0 designates the elastic modulus for a material with no chemical and mechanical deterioration.

THE MATHEMATICAL SIMULATION MODEL

For the numerical simulation of the storage casks, a 3D coupled thermo-hydro-mechanical model, called NEWCON3D, was adopted.

In this code concrete is treated as a multiphase system where the voids of the skeleton are partly filled with liquid and partly with a gas phase (Gawin et al., 1999; Baggio et al., 1995). The liquid phase consists of bound water (or adsorbed water), which is present in the whole range of water contents of the medium, and capillary water (or free water), which appears when water content exceeds so-called solid saturation point S_{ssp}, i.e. the upper limit of the hygroscopic region of moisture content. The gas phase, i.e. moist air, is a mixture of dry air (non-condensable constituent) and water vapour (condensable gas), and is assumed to behave as an ideal gas.

The approach taken here is to start from a phenomenological model (Majorana et al., 1998; Majorana et al., 2004, Salomoni et al., 2007) originally developed by Bažant and co-authors, e.g. (Bazănt et al., 1978), in which mass diffusion and heat convection-conduction equations are written in terms of relative humidity, to an upgraded version in which its non-linear diffusive nature is maintained as well as the substitution of the linear momentum balance equations of the fluids with a constitutive equation for fluxes, but new calculations of thermodynamic properties for humid gases are implemented to take into account different phases as well as high ranges of both pressure and temperature. Additionally, Darcy's law is modified when describing gas flow through concrete.

With regard to the mechanical field, when considering creep and damage respectively, Model B3 (Bazănt et al., 2000) and Mazars' damage law (Mazars et al., 1986) with non-local correction have been chosen and implemented.

Hygro-thermo-mechanical model

The coupled system of differential equations for dealing with humidity diffusion and heat transport can be written in the form (Majorana et al., 1998; Majorana et al., 2004; Salomoni et al., 2007):

$$\mathrm{k}\frac{\partial \mathrm{h}}{\partial \mathrm{t}} - \nabla^{\mathrm{T}}\mathbf{C}\nabla \mathrm{h} - \frac{\partial \mathrm{h_s}}{\partial \mathrm{t}} - \mathrm{K}\frac{\partial \mathrm{T}}{\partial \mathrm{t}} + \overline{\alpha}\mathbf{m}^{\mathrm{T}}\frac{\partial \boldsymbol{\varepsilon}}{\partial \mathrm{t}} = 0 \tag{5}$$

$$\rho \mathrm{C_q}\frac{\partial \mathrm{T}}{\partial \mathrm{t}} - \nabla^{\mathrm{T}}\boldsymbol{\Lambda}\nabla \mathrm{T} - \frac{\partial \mathrm{Q_h}}{\partial \mathrm{t}} = 0 \tag{6}$$

where k is the cotangent of the isotherm slope, **C** is the diagonal (isotropic) matrix of relative humidity diffusivity diagonal matrix, $\mathrm{dh_s}$ the self-desiccation, K the hygrothermal coefficient, $\mathbf{m} = \{1 \quad 1 \quad 1 \quad 0 \quad 0 \quad 0\}^{\mathrm{T}}$, $\overline{\alpha} = \left(\frac{\partial \mathrm{h}}{\partial \boldsymbol{\varepsilon}_{\mathrm{v}}}\right)\Big|_{\mathrm{T,w}}$ equals the change in h due to unit change of volumetric strain ε_v at constant moisture content w and temperature T, ρC_q is the thermal capacity, $\boldsymbol{\Lambda}$ the thermal conductivity diagonal matrix and Q_h the outflow of heat per unit volume of solid. The last term in Equation 5 represents the coupling term for connecting hygro-thermal and mechanical responses.

The linear momentum balance equation for the entire multiphase medium, neglecting inertial forces, reads

$$div\boldsymbol{\sigma} \quad + \quad \rho^{m}\mathbf{g} = 0 \tag{7}$$

where $\boldsymbol{\sigma}$ is the total stress tensor, ρ^m is the mass density of the multiphase medium (concrete plus water species) and **g** is the gravitational acceleration.

Finite Element Discretization

The application, within the numerical code NEWCON3D, of a standard finite element discretization in space of Equations 5-7 results in:

$$\begin{bmatrix} \mathbf{K} & \mathbf{HU} & \mathbf{TU} \\ \mathbf{L}^T & \mathbf{I} & \mathbf{TP} \\ \mathbf{0} & \mathbf{TH} & \mathbf{TS} \end{bmatrix} \begin{Bmatrix} \dot{\bar{\mathbf{u}}} \\ \dot{\bar{\mathbf{h}}} \\ \dot{\bar{\mathbf{T}}} \end{Bmatrix} + \begin{bmatrix} \mathbf{0} & \mathbf{0} & \mathbf{0} \\ \mathbf{0} & \mathbf{Q} & \mathbf{0} \\ \mathbf{0} & \mathbf{0} & \mathbf{TR} \end{bmatrix} \begin{Bmatrix} \bar{\mathbf{u}} \\ \bar{\mathbf{h}} \\ \bar{\mathbf{T}} \end{Bmatrix} = \begin{Bmatrix} \dot{\mathbf{f}} + \mathbf{c} \\ \dot{\mathbf{HG}} \\ \dot{\mathbf{TG}} \end{Bmatrix} \tag{8}$$

where $\bar{\mathbf{u}}$, $\bar{\mathbf{h}}$ and $\bar{\mathbf{T}}$ are the nodal values of the basic variables and where **HU** and **TU** account for shrinkage and thermal dilation effects, respectively; $\mathbf{L}^T$ and **TP** are the coupling matrices representing the influence of the mechanical and thermal field on the hygral one, respectively; **Q** is the diffusivity matrix accounting for sorption-desorption isotherms; **TH** the coupling matrix between the hygral and thermal fields in terms of capacity; **TS** the matrix of heat capacity; **TR** the matrix of thermal transmission including the convective term; **c** the matrix accounting for creep; **HG** the matrix of humidity variation due to drying and **TG** accounts for heat fluxes. For further explanations of the above terms the reader is referred to (Salomoni et al., 2009; Xotta et al., 2013).

NUMERICAL ANALYSES

In this section, different simulations were performed to study a cylindrical DCSS subjected to realistic hygral-thermal loads and to self-weight for more than 40 years. The purpose was to determine the long-term behavior of the cask and possible environmental damage scenarios due to different loads acting simultaneously.

To this end a cylindrical containment structure was considered made of a concrete outer-pack reinforced on the outer surface by rebars and a steel liner on the inside. The height is 5.7 m, the outer diameter is 3.5 m and the cylinder wall is 0.75 m thick. A 3D FE mesh of the cask and the corresponding discretization adopted for the axisymmetric studies are shown in Figure 1. The main material properties for the analyses are listed in Table 1; as expected the steel is considered to remain linearly elastic, characterized by higher thermal properties and zero permeability (no shrinkage) while concrete is assumed to behave as a visco-elastic material subject to elastic damage, i.e. degradation of stiffness and strength according to Mazars, 1986.

With regard to the environmental conditions, the relative humidity, RH, of concrete is assumed to be initially at 80% RH, whereby the cask is exposed to drying for the entire period of 40 years assuming that the outside relative humidity remains at 50% RH. For the thermal load, it is assumed that the steel liner is subjected on the inside to a thermal ramp from 20°C to 80°C in less than one day, in order to simulate the heating due to the presence of the fuel basket on the inside. This temperature is maintained constant until the end of the analysis. The entire cask structure is assumed to be initially at 20°C and subjected to an ambient outside temperature which remains at that level using convective boundary conditions.

With regard to the mechanical loading, no external forces are considered except for self-weight of the concrete cask (assuming the fuel canister is not connected to the dry cask); in short, only self-weight of the structure is taken into consideration.

Table 1: Material data for the dry cask storage system.

Material	Elastic Modulus [MPa]	Poisson's Ratio	Reference Diffusivity along X,Y[mm^2/d]	Unrestrained Shrinkage	Thermal Conductivity along X,Y [N/d·K]	Thermal expansion coefficient	Thermal Capacity [N/mm^2·K]
Concrete	30000	0.20	20	0.004	118368	0.00001	2.112
Stainless Steel	200000	0.28	--	--	1399680	0.0000157	3.9
Rebar	200000	0.25	--	--	4406400	0.000015	3.9

Figure 2 shows the distribution of relative humidity evolution in the concrete outer-pack during

drying. The hygro-thermo-mechanical analysis illustrates accelerated drying due to the thermal ramp at the inside liner (H-T-M Analysis) and a relative humidity RH distribution which decreases very slowly in a uniform manner when no temperature gradient is included (H-M Analysis). In fact, in the hygro-mechanical case, the relative humidity reduces to 75% RH only after 40 years.

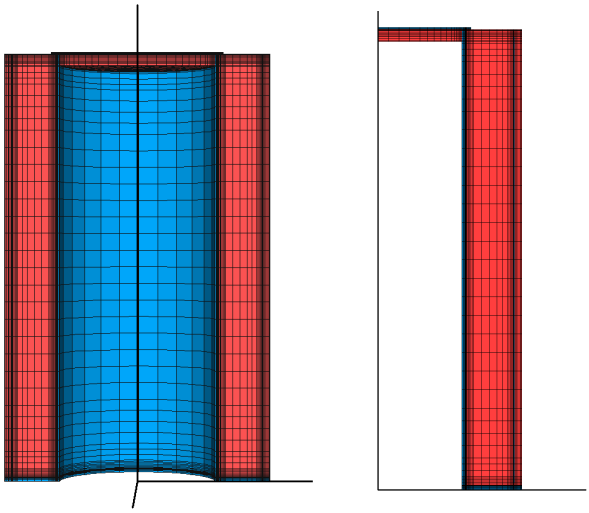

Figure 1: 3D FE mesh of the cask and the corresponding axisymmetric section.

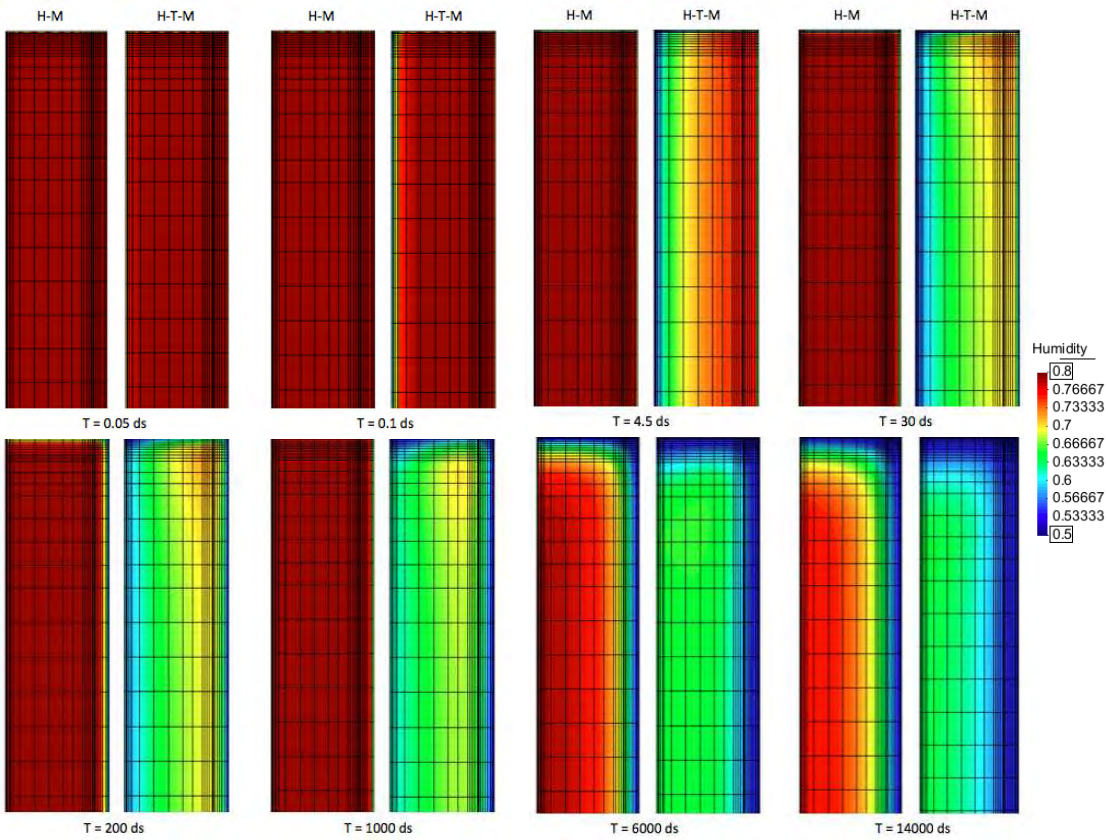

Figure 2: Relative humidity evolution of the concrete outer pack for the hygro-mechanical (H-M) and hygro-thermo-mechanical conditions (H-T-M) (Only the upper part of the axisymmetric section is shown here for better visualization).

For a better comprehension of the time histories, let us consider three representative nodes in the dry cask (one node close to the steel liner (node 1480) and the other two nodes, in the center top segment of the cask). Comparing the relative humidity histories of the two different analyses (see Figure 3), other interesting observations may be made. In fact for the hygro-thermo-mechanical case, considering nodes 1480 and 1798 closer to the inside liner, the relative humidity is firstly drastically reduced by the thermal ramp effect and then, due to the drying from outside there is a slight increase in relative humidity (especially for the node 1480 close to the steel liner), that constitutes a physical obstacle to humidity transport reaching at the end a steady state condition. For node 2116 the relative humidity history exhibits a vertical shift when the internal heating is included as compared to the case without heating.

With regard the thermal behavior of the cask, the temperature distribution is shown in Figure 4, whereby a steady state is reached in a relatively short time.

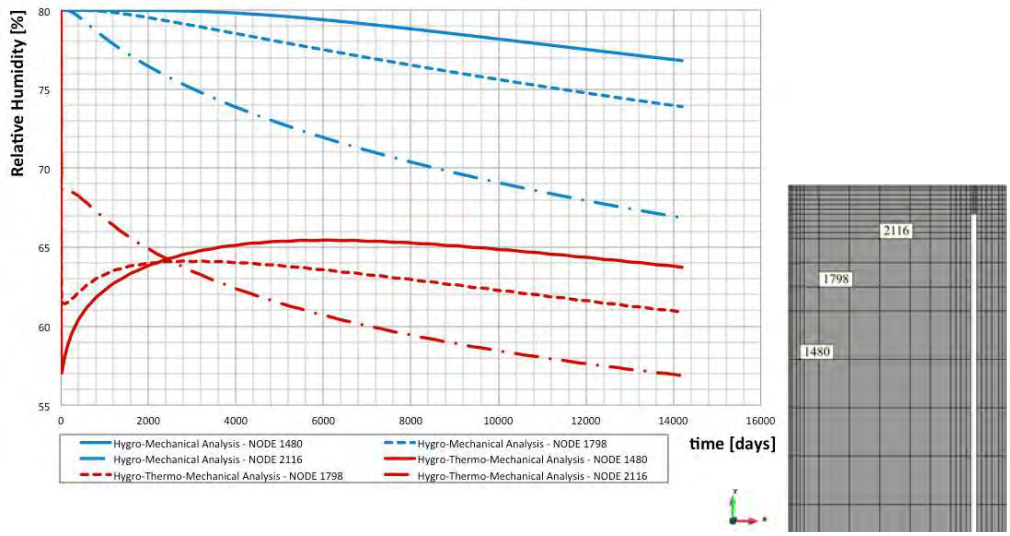

Figure 3: R.H. distribution for three representative nodes in the cask structure.

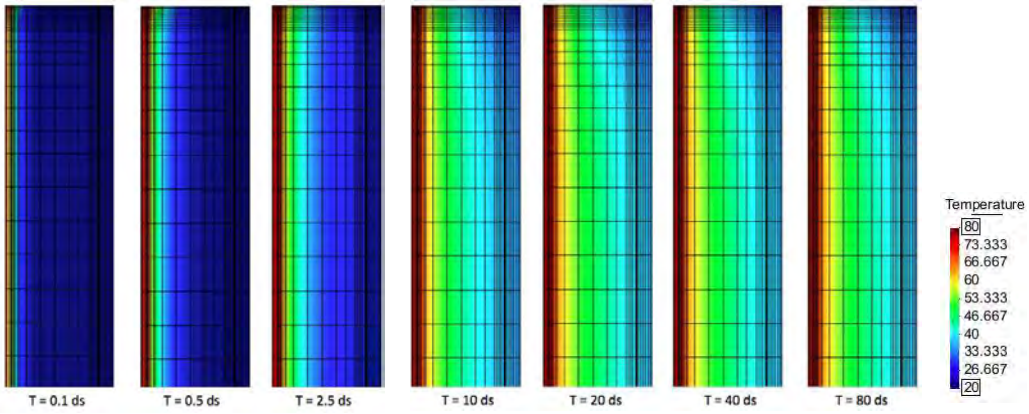

Figure 4: Evolution of temperature for the dry cask (only the upper part of the axisymmetric section is shown here for better visualization).

Recalling the linear momentum balance equation $div(\boldsymbol{\sigma}) + \mathbf{b} = \mathbf{0}$, this expands into the following differential format of quasi-static equilibrium

$$div\left((1-D)\mathbf{E}(\boldsymbol{\varepsilon} - \boldsymbol{\varepsilon}_S - \boldsymbol{\varepsilon}_T)\right) \quad + \quad \rho^m \mathbf{g} = 0 \tag{9}$$

where D designates the Mazars' damage parameter of effective tensile strain (see Mazars, 1986), while

$\boldsymbol{\varepsilon}$ is the total strain derived from the symmetric displacement gradient, $\boldsymbol{\varepsilon}_S$ is the volumetric strain due to shrinkage and $\boldsymbol{\varepsilon}_T$ the volumetric strain due to thermal expansion.

The components of $\boldsymbol{\varepsilon}_S$ and $\boldsymbol{\varepsilon}_T$ relate the shrinkage and thermal strains to the gradients of RH, Δh, and temperature, ΔT:

$$\Delta\boldsymbol{\varepsilon}_S = \mathbf{k}\Delta h \qquad \Delta\boldsymbol{\varepsilon}_T = \boldsymbol{\alpha}\Delta T \tag{10}$$

where $\mathbf{k}$ is the isotropic tensor of shrinkage and $\boldsymbol{\alpha}$ is the isotropic tensor of thermal dilation.

Consequently, if we are interested in the mechanical degradation of the cask due to environmental effects, we need to activate redistribution of the initially compressive stress state under self-weight to mobilize damage in form of tensile cracking:

$$div(\Delta\boldsymbol{\sigma}) \neq 0 \tag{11}$$

In fact, if the cask is free to expand or to shrink, there will be no kinematic restraint and the divergence of stress is the sole source of hygro-thermal stresses and therefore mechanical damage in form of e.g. tensile microcracking. In short, mechanical damage will take place only if the critical tensile strain condition is being reached due to redistribution of stress $div(\Delta\boldsymbol{\sigma}) \neq 0$.

Considering only creep under self-weight and drying shrinkage without kinematic constraints, the stresses remain very low and consequently no damage can be seen. Instead, if a large thermal ramp is considered, deterioration of concrete due to the temperature gradient and the mismatch between steel and concrete takes place in form of tensile cracking. Indeed, if the test structure were just concrete, if no thermal gradient were acting, or if heating was applied really slowly, no mechanical deterioration may be expected; in contradistinction, outside fire conditions would lead to a worst case environmental scenario. Figure 5 illustrates the time evolution of tensile damage parameter for the cask section under hygro-thermo-mechanical conditions. This figure clearly shows that damage develops at the interface between the two materials starting at the top-left interface between the liner and the concrete. It propagates along the interface over the entire height of the cask and it finally reaches the outside surface of the cask at the bottom right. Only a narrow zone is subjected to deterioration where the damage parameter reaches a value equal to one, D=1, indicating full degradation of tensile stress due to softening. This effect is severely localized at the interface on the top-left corner indicating delamination and cracking between the liner and concrete.

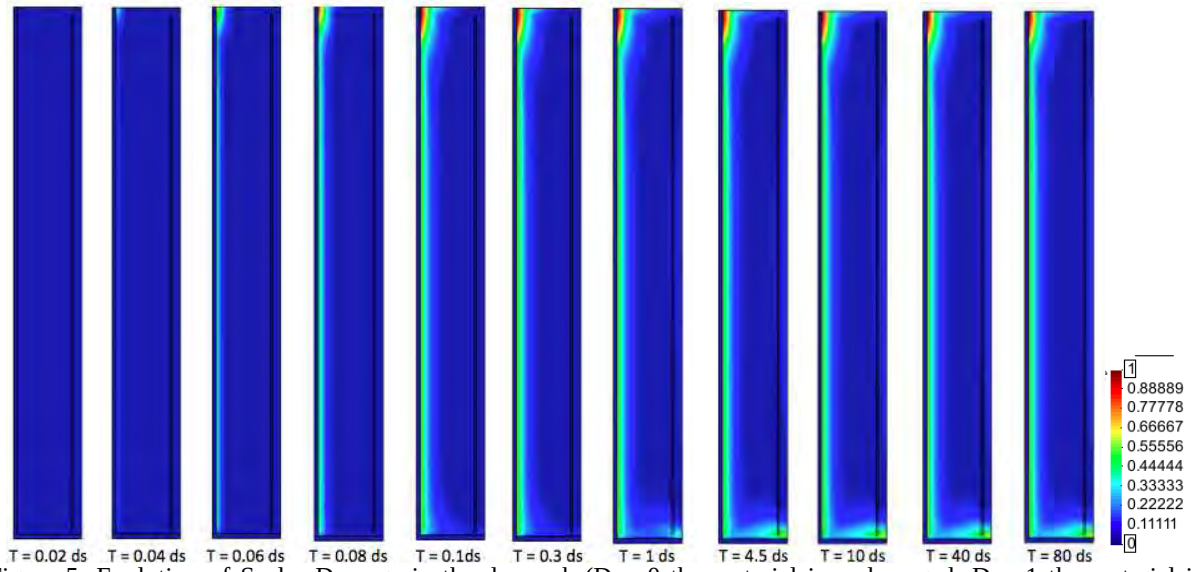

Figure 5: Evolution of Scalar Damage in the dry cask (D = 0 the material is undamaged; D = 1 the material is completely damaged due to excessive tensile straining, Mazars, 1986).

CONCLUSIONS

In this presentation possible damage scenarios are studied of a cylindrical DCSS subjected to realistic hygral-thermal loads and to self-weight for a duration of 40 years. For the simulations a coupled thermo-hygro-mechanical finite element code is used, which treats concrete as a multiphase system.

The results highlight how the thermal gradients lead to be the worst scenario among the other load cases considered in this paper, and it may affect the long-term performance of the casks. Indeed, under creep and shrinkage due self-weight the stress level remains very low and, consequently, no damage was observed; if a large thermal ramp is considered and thus a significant temperature gradient develops, then tensile softening in form of cracking develops in the concrete outer-pack due to the temperature gradient and the mismatch between steel and concrete. However the region of damage is restricted to the proximity of the steel – concrete interface indicating delamination tendencies due to the mismatch between the liner and the creep deformations of the concrete outer-pack.

REFERENCES

Baggio, P., Majorana, C.E. and Schrefler, B.A. (1995). "Thermo-hygro-mechanical analysis of concrete," *International Journal for Numerical Methods in Fluids* 20, 573-595.

Bangert, F., Kuhl, D. and Meschke, G. (2004). "Chemo-hygro-mechanical modelling and numerical simulation of concrete deterioration caused by alkali–silica reaction," *Int. J. Numer. Anal. Meth. Geomech* 28 (78), 689-714.

Bazănt, Z.P. and Steffens, A. (2000). "Mathematical model for kinetics of alkali–silica reaction in concrete," *Cement and Concrete Research* 30, 419-428.

Bazănt, Z.P. and Meyer, C. (2000). "Fracture mechanics of ASR in concretes with waste glass particles of different size," ASCE *Journal of Engineering Mechanics* 126, 226-232.

Bažant, Z.P. and Thonguthai, W. (1978). "Pore pressure and drying of concrete at high temperature," *Journal of the Engineering Mechanics* Division 104, 1058-1080.

Bažant, Z.P. and Baweja, S. (2000). "Creep and shrinkage prediction model for analysis and deign of concrete structures: Model B3," in *Adam Neville Symposium: Creep and Shrinkage – Structural Design Effects*, ACI SP – 194, 1-83.

Comi, C., Fedele, R. and Perego, U. (2009). "A chemo-thermo-damage model for the analysis of concrete dams affected by alkali-silica reaction," *Mechanics of Materials* 41, 210-230.

Dron, R. and Brivot, F. (1992). "Thermodynamic and kinetic approach to the alkali-silica reaction. Part 1: Concepts," *Cement and Concrete Research* 22 (5), 941-948

Dron, R. and Brivot, F. (1993). ". Thermodynamic and kinetic approach to the alkali-silica reaction. Part 2: Experiment," *Cement and Concrete Research*, 23 (1), 93-103.

Gawin, D., Majorana, C.E. and Schrefler, B.A. (1999). "Numerical analysis of hygro-thermal behaviour and damage of concrete at high temperature," *Mechanics of Cohesive Frictional Materials* 4, 37-74.

Isteita, M.H. (2009). "The effect of Thermal Conduction on Chloride Penetration in Concrete." M.S. Thesis, University of Colorado at Boulder.

Majorana, C.E., Salomoni, V. and Schrefler, B.A. (1998). "Hygrothermal and mechanical model of concrete at high temperature," *Materials and Structures* 31 (210), 378-386.

Majorana, C.E. and Salomoni, V.A. (2004). "Parametric analyses of diffusion of activated sources in disposal forms," *Journal of Hazardous Materials* A113, 45-56.

Mazars, J. (1986). "A Description of Micro and Macro-scale Damage of Concrete structures," *Engineering Fracture Mechanics* 25 (5-6), 729-737.

Pesavento, F., Gawin, D., Wyrzykowski, M., Schrefler, B.A. and Simoni, L. (2012). "Modeling alkali–silica reaction in non-isothermal, partially saturated cement based materials," *Comput. Methods Appl. Mech. Engrg.* 225 (228), 95-115.

Saetta, A., Schrefler, B.A. and Vitaliani, R. (1993). "The carbonation of concrete and the mechanism of moisture, heat and cabon dioxide flow through porous materials," *Cement and Concrete Research* 25

(8), 1703-1712.

Salomoni, V.A., Mazzucco, G. and Majorana, C.E. (2007). "Mechanical and durability behavior of growing concrete structures," *Engineering Computations* 24 (5), 536-561.

Salomoni, V.A., Majorana, C.E., Mazzucco, G., Xotta, G., and Khoury, G.A. (2009). "Multiscale modelling of Concrete as a Fully Coupled Porous Medium," in Sentowski J.T (Ed.), *Concrete Materials: Properties, Performance and Applications*, Ch. 3, NOVA Science Publishers, NY, USA, 171-231.

Stanton, T. E. (1940). "Expansion of concrete through reaction between cement and aggregate," *Proc.* ASCE 66, 1781-1811.

Steffens, A., Li, K. and Coussy, O. (2003). "Ageing approach to water effect on alkali-silica reaction," *Degradation of Structures, Journal of Engineering Mechanics* 129, 50-59.

Ulm, F.J., Coussy, O., Kefei, L. and Larive, C. (2000). "Thermo-chemo-mechanics of ASR expansion in concrete structures," *Journal of Engineering Mechanics* 126, 233-242.

Xotta, G., Salomoni, V.A. and Majorana, C.E. (2013). "Thermo-hygro-mechanical meso-scale analysis of concrete as a viscoelastic-damaged material," *Engineering Computations* 30 (5).